NeuroImage: Clinical 2 (2013) 569–580

Contents lists available at ScienceDirect

NeuroImage: Clinical

journal homepage: www.elsevier.com/locate/ynicl

Evaluation of white matter myelin water fraction in chronic stroke ☆

M.R. Borich [a], A.L. MacKay [b,c], I.M. Vavasour [b], A. Rauscher [b,d,e], L.A. Boyd [a,e,*]

[a] Department of Physical Therapy, University of British Columbia, Canada
[b] Department of Radiology, University of British Columbia, Canada
[c] Department of Physics and Astronomy, University of British Columbia, Canada
[d] UBC MRI Research Centre, University of British Columbia, Canada
[e] Brain Research Centre, University of British Columbia, Canada

ARTICLE INFO

Article history:
Received 21 January 2013
Received in revised form 11 April 2013
Accepted 11 April 2013
Available online 21 April 2013

Keywords:
Stroke
Myelin water fraction
T_2 relaxation
Motor recovery
White matter

ABSTRACT

Multi-component T_2 relaxation imaging (MCRI) provides specific *in vivo* measurement of myelin water content and tissue water environments through myelin water fraction (MWF), intra/extra-cellular water fraction (I/EWF) and intra/extracellular and global geometric mean T_2 (GMT_2) times. Quantitative MCRI assessment of tissue water environments has provided new insights into the progression and underlying white matter pathology in neural disorders such as multiple sclerosis. It has not previously been applied to investigate changes in white matter in the stroke-affected brain. Thus, the purposes of this study were to 1) use MCRI to index myelin water content and tissue water environments in the brain after stroke 2) evaluate relationships between MWF and diffusion behavior indexed by diffusion tensor imaging-based metrics and 3) examine the relationship between white matter status (MWF and fractional anisotropy) and motor behavior in the chronic phase of stroke recovery. Twenty individuals with ischemic stroke and 12 matched healthy controls participated. Excellent to good test/re-test and inter-rater reliability was observed for region of interest-based voxelwise MWF data. Reduced MWF was observed in whole-cerebrum white matter ($p < 0.001$) and in the ipsilesional ($p = 0.017$) and contralesional ($p = 0.037$) posterior limb of internal capsule (PLIC) after stroke compared to whole-cerebrum and bilateral PLIC MWF in healthy controls. The stroke group also demonstrated increased I/EWF, I/E GMT_2 and global GMT_2 times for whole-cerebrum white matter. Measures of diffusion behavior were also significantly different in the stroke group across each region investigated ($p < 0.001$). MWF was not significantly correlated with specific tensor-based measures of diffusion in the PLIC for either group. Fractional anisotropy in the ipsilesional PLIC correlated with motor behavior in chronic stroke. These results provide novel insights into tissue-specific changes within white matter after stroke that may have important applications for the understanding of the neuropathology of stroke.

1. Introduction

Stroke is the leading cause of long-term severe disability in the U.S. (Minino et al., 2011) and nearly half of all stroke survivors live with a disability level characterized as moderate to severe (Kelly-Hayes et al., 2003). However, stroke mortality rates are declining, resulting in a greater number of individuals living with significant disability with limited effective treatment options to regain function (Gillum et al., 2011). Increasing evidence has indicated that stroke-related damage to white matter brain regions is related to trajectory and level of recovery (Borich et al., 2012a; Jang et al., 2005; Stinear et al., 2007). White matter is composed of both neuronal axons and supporting glial cells and it is currently unclear how specific components of white matter tissue contribute to recovery from stoke. In rodent models of both acute (Tanaka et al., 2003) and chronic (Chida et al., 2011) ischemic stroke, white matter degeneration is present, while remyelination is positively associated with recovery (Chida et al., 2011). In myelinated axons, normal neural impulse conduction relies on the insulating properties of myelin and disturbances to the myelin sheath can cause severe impairments in motor and sensory functioning (Readhead et al., 1987). In many demyelinating disorders, the primary event is a breakdown of the blood–brain barrier (Baumann and Pham-Dinh, 2001), which also occurs in stroke where white matter tissue is particularly susceptible to ischemic-induced damage (Dewar et al., 1999).

Despite the importance of myelin to normal neural function, relatively little is known about changes in myelin following stroke in humans. This knowledge gap stems in part from technological limitations that until recently prevented the whole-brain imaging of myelin *in vivo*. However, non-invasive imaging techniques that have emerged are sensitive to detect *in vivo* changes in cerebral myelin, enabling

* Corresponding author at: University of British Columbia, Department of Physical Therapy, 212-2177 Wesbrook Mall, Vancouver, British Columbia V6T 1Z3, Canada. Tel.: +1 604 827 3369; fax: +1 604 822 1870.
E-mail address: lara.boyd@ubc.ca (L.A. Boyd).

2213-1582/$ – see front matter © 2013 The Authors. Published by Elsevier Inc. All rights reserved.
http://dx.doi.org/10.1016/j.nicl.2013.04.006

evaluation of these changes associated with white matter abnormalities in clinical populations.

Multi-component T_2 relaxation imaging (MCRI) is a non-invasive, *in vivo* magnetic resonance technique used to quantify water content in brain tissue compartments. A typical T_2 distribution in the normal human brain is characterized by three chief components determined by the proton signal relaxation time: 1) a long T2 component (>2 s) that is attributed to cerebral spinal fluid, 2) an intermediate T2 component (~80 ms) has been assigned to intra/extracellular water, and 3) a short T2 component (<40 ms) that reflects water trapped between myelin lipid bilayers (Mackay et al., 1994; Menon and Allen, 1991; Stewart et al., 1993; Whittall et al., 1997). Specifically, MCRI provides a quantitative measure of myelin (myelin water fraction or MWF) in both abnormal and normal-appearing regions of white matter tissue. Importantly, recent advances in multi-echo pulse sequences now offer increased spatial coverage allowing for near whole-brain imaging in clinically feasible acquisition times (Deoni et al., 2008; Lenz et al., 2012; Nguyen et al., 2012; Oh et al., 2006; Prasloski et al., 2012b).

Measurement of MWF based on the analysis of the T_2 distribution has been validated as an *in vivo* marker for myelin content in the human brain (Laule et al., 2006, 2008). In guinea pig (Gareau et al., 1999, 2000) and rat (Webb et al., 2003), white matter T_2 distributions are multi-compartmental and the short T_2 component correlates with histological measures of myelin. Formalin-fixed human brains yield T_2 distributions similar to those found *in vivo*, and histopathological studies show strong correlations (mean 'r's = 0.67 to 0.78) between MWF and staining for myelin (Laule et al., 2006, 2008; Moore et al., 2000). Studies of individuals with MS reveal decreased MWF in both lesions and normal appearing white matter NAWM (Laule et al., 2004; Vavasour et al., 1998). MCRI measurements of myelin also appear to relate to the severity of clinical signs indexed by the Expanded Disability Status Scale in individuals with MS (Laule et al., 2011). MCRI can also provide unique insights into the intra/extracellular environment. In MS, prolonged intra/extracellular T_2 relaxation times have been observed in white matter lesions compared to NAWM (Laule et al., 2007). Also, elevated mean T_2 times, likely reflecting vascular edema and tissue water uptake, have been observed in both the acute and sub-acute (<6 days) phases of stroke recovery (Noguchi et al., 1997; Siemonsen et al., 2009, 2012).

In stroke, diffusion imaging techniques have been used to evaluate microstructural changes in white matter in the acute, sub-acute and chronic phases of recovery. This work has advanced the understanding of the contributions of white matter microstructural status to recovery after stroke (Schaechter et al., 2009; Stinear et al., 2007; Wang et al., 2012). Specifically, diffusivity perpendicular to the primary axis of diffusion (radial diffusivity or RD) has been hypothesized to be influenced by the degree of myelination (Song et al., 2002, 2003) and may have the potential to differentiate between axonal and glial damage after stroke (Wang et al., 2012). Though diffusion-derived measurements of white matter have shown sensitivity to change in patient populations, especially fractional anisotropy (FA) (Borich et al., 2012a; Jang et al., 2005; Stinear et al., 2007), they are relatively non-specific regarding pathological changes in intra-voxel tissue structure. For example, Wang et al. (2011) showed that demyelination, edema and inflammation each resulted in increased RD, a diffusion-based measure commonly associated with myelin status (Wang et al., 2011). Other diffusion methods are becoming available (Assaf and Basser, 2005; Hui et al., 2008; Jeurissen et al., 2011; Wang et al., 2011) that may dissociate these effects but they have not been validated in humans.

Given the established relationship between normal neural function and myelin status along with evidence of white matter damage following stroke using diffusion imaging, the principal aim of this investigation was to quantify myelin and intra/extracellular T_2 relaxation *in vivo* in the human brain after stroke. Because this is the first report of myelin status in individuals with stroke, we also conducted analyses to ensure test/re-test reliability and to assess intra-rater reliability of our regions of interest approach. A secondary aim was to determine if myelin status, indexed by MWF, correlated with standard DTI-based measures of white matter status. A tertiary aim was to examine if MWF and/or FA related to measures of motor behavior in chronic stroke.

2. Materials and methods

2.1. Participant characteristics

Twenty individuals presenting with a clinically-significant, first-time, chronic (>6 months) ischemic infarct (Fig. 1) with movement-related deficits and twelve age-matched healthy controls were recruited. Individuals who were at least 6 months post-stroke were recruited to avoid confounding spontaneous neural changes immediately following stroke (Cramer, 2008). Consent for each participant was obtained according to the Declaration of Helsinki; the clinical research ethics boards at the University of British Columbia approved all aspects of the study. For stroke participants, upper extremity physical impairment was quantified using the upper extremity portion of the Fugl-Meyer (FM) motor scale (0–66, higher scores indicate less physical impairment) for each stroke participant (Fugl-Meyer et al., 1975) and each FM assessment was conducted by a single licensed physical therapist (M.R.B). Participant characteristics are summarized in Table 1.

Exclusion criteria for the stroke and healthy control groups included: (1) signs of dementia (score < 24 on the Montreal Cognitive Assessment) (Nasreddine et al., 2005); (2) left hand dominance (Oldfield, 1971); (3) any contraindications to MRI; or (4) history of seizure/epilepsy, head trauma, a major psychiatric diagnosis, neurodegenerative disorder or substance abuse. For the healthy control group, participants exhibiting any frank or clinically evident signs of neurological impairment or disease were also excluded from this study (Lundy-Ekman, 1998).

2.2. In vivo magnetic resonance acquisition

MR acquisition was conducted at the UBC MRI Research Centre on a Philips Achieva 3.0 T whole body MRI scanner (Phillips Healthcare, Best, NL). The following scans were collected: (1) 3D T_1 turbo field echo (TFE) scan (TR = 7.4 ms, TE = 3.7 ms, flip angle $\theta = 6°$, FOV = 256 × 256 mm, 160 slices, 1 mm slice thickness, scan time = 3.2 min), (2) 60-orientation diffusion weighted scan with a single shot echo-planar imaging (EPI) sequence (TR = 7013 ms, TE = 60 ms, FOV = 224 × 224 mm, 70 slices, 2.2 mm slice thickness, voxel dimension = 2.2 mm^3, b = 700 s/mm^2, scan time = 7.4 min) and 5 b = 0 s/mm2 images, and (3) whole-cerebrum 32-echo three-dimensional gradient- and spin-echo (3D GRASE) for T2 measurement (TR = 1000 ms, echo times = 10,20,30,…,320 ms, 20 slices acquired at 5 mm slice thickness, 40 slices reconstructed at 2.5 mm slice thickness (*i.e.* zero filled interpolation), slice oversampling factor = 1.3 (*i.e.* 26 slices were actually acquired but only the central 20 were reconstructed), in-plane voxel size = 1 × 1 mm, SENSE = 2, 232 × 192 matrix, receiver bandwidth = 188 kHz, axial orientation, acquisition time = 14.4 min) (Prasloski et al., 2012b).

2.3. Magnetic resonance data processing and analysis

T_2 relaxation analysis used a non-negative least-squares (NNLS) approach (Whittall and Mackay, 1989) with the extended phase graph algorithm (Prasloski et al., 2012a) to partition the T_2 signal using an unbiased approach based on the signal characteristics into short (15-40 ms), intermediate (40–200 ms) and long (>1500 ms) components using in-house software code (MATLAB R2010b, The MathWorks, Inc.) developed at the University of British Columbia (Fig. 2). Global GMT_2 was defined as the mean T_2 on a log scale between 15 ms and 2000 ms. Myelin water fraction (MWF) was defined as the sum of the amplitudes within the short T_2 component (15–

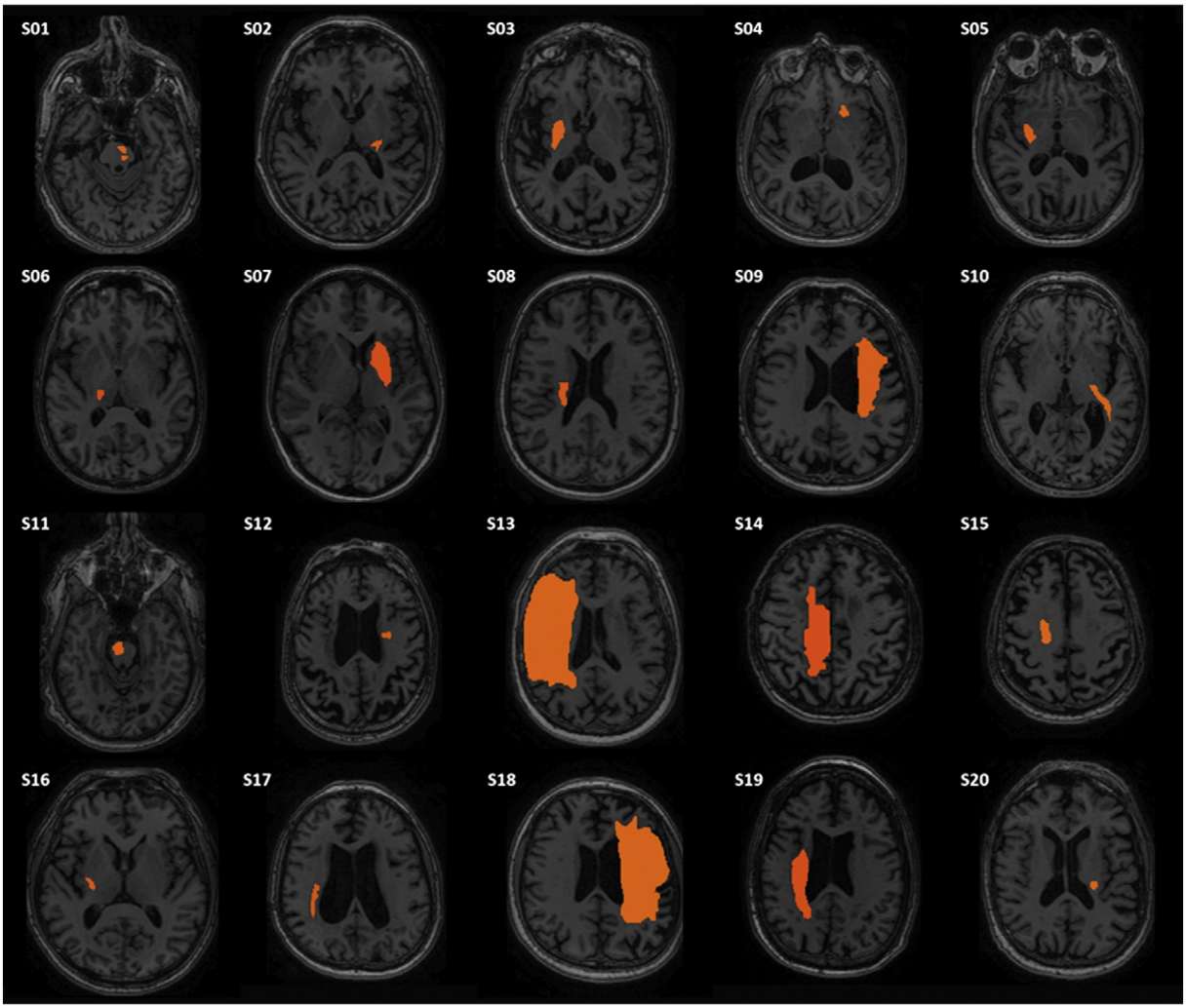

Fig. 1. T_1 image of axial slice in which stroke lesion (outlined in red) area is largest for each participant in the stroke group.

40 ms) divided by the sum of the amplitudes for the total T_2 distribution. Geometric mean T_2 (I/E GMT_2) of intra/extracellular water was defined as the mean T_2 on a log scale between 40 ms and 200 ms. The intra/extracellular water fraction (I/EWF) was represented as the sum of the amplitudes within the middle T_2 component (40–200 ms) divided by the sum of the amplitudes for the total T_2 distribution.

Voxel-based maps (Fig. 3) were produced for each participant to evaluate MWF, I/E GMT2, I/EWF and GMT2 in desired regions of interest (ROI). These ROIs included: whole-cerebrum normal appearing white matter (NAWM) and the posterior limb of the internal capsule (PLIC) bilaterally. Tools in the FMRIB Software Library (FSL) (Smith et al., 2004) were used generate the ROI masks. Initially, fractional anisotropy maps were generated using the dtifit component of FDT (Smith et al., 2004). These maps were then co-registered to the first echo of the T2 scan using an affine 12 parameter model in FLIRT (Jenkinson et al., 2002). The co-registered images were automatically segmented into gray matter, white matter and cerebrospinal fluid using FAST (Zhang et al., 2001). The white matter segmentation mask was eroded by one voxel to remove any brain edge artifacts or subcortical gray matter tissue. Successful erosion was visually confirmed for each mask, which was subsequently used as the NAWM mask. Cross-sectional ROI masks were manually delineated for the PLIC bilaterally for each subject using FSLView. Areas of infarct were automatically excluded from whole brain NAWM ROIs and manually excluded from ipsilesional PLIC ROIs. Complete disruption of the affected PLIC was not observed for any participant, however, 41% (9/22) of participants had evidence of partial lesion encroachment within the ipsilesional PLIC.

Diffusion imaging data were first visually inspected for excessive motion artifact or instrumental noise using quality assurance tools available in the diffusion MRI software package ExploreDTI (www.exploredti.com) (Leemans et al., 2009). Less than 1% of images were removed across all subjects. Imaging data were then corrected for motion and distortion. During motion correction, signal intensity was modulated and the b-matrix was rotated (Leemans and Jones, 2009). Tensor estimation was performed using the RESTORE (Robust Estimation of Tensor Outlier Rejection algorithm) (Chang et al., 2005) and subsequent data were processed and analyzed in native space. Whole-brain fiber tractography was performed using a deterministic streamline approach. Fractional anisotropy (FA) threshold for initiation and continuation of tract reconstruction was 0.2 and tract-turning angle threshold was set to 30°. To isolate fiber tracts within the PLIC, a tract segment analysis approach was used (Fig. 4). ROIs were placed in the axial plane using the level of the anterior commissure as the inferior border and the inferior aspect of the corona radiata as the superior border. Fiber tracts were then reconstructed within the circumscribed volume and mean values for FA, mean diffusivity (MD), axial diffusivity (AD) and RD were extracted to evaluate diffusion behavior within tracts in the PLIC. MD represents diffusion behavior averaged across the three principal eigenvalues of the tensor ellipsoid ($\lambda_1 + \lambda_2 + \lambda_3 / 3$). AD measures diffusion along

Table 1
Participant characteristics.

Participant ID	Age (y)	Gender	Post-stroke duration (mo)	MOCA (/30)	FM score (/66)	WMFT affected (s)	WMFT unaffected (s)	Grip strength affected (kg)	Grip strength unaffected (kg)
Stroke									
1	74	M	142	27	60	1	0.81	29	47
2	61	F	83	27	56	1.6	1.19	9	15
3	85	M	13	25	60	1.72	1.53	22	24
4	67	M	82	25	59	0.83	0.68	29	37
5	62	M	41	28	23	120	0.85	11	40
6	66	F	27	30	58	1.46	1.24	18	27
7	50	F	37	26	63	1.01	0.85	28	30
8	56	F	27	30	35	1.63	0.83	16	30
9	59	M	270	28	55	2.5	1.53	17	31
10	76	M	81	29	62	0.96	0.84	41	36
11	71	M	20	28	58	1.22	1.08	28	40
12	65	F	67	30	62	1.22	1.01	23.3	28
13	76	M	155	26	49	4.29	1.28	16.6	31
14	64	F	94	26	56	1.18	1.27	20	24
15	82	M	12	26	59	1.56	1.25	17.3	30
16	69	F	15	28	57	1.14	0.82	16	44
17	60	M	23	29	54	1.43	1.59	12.3	14
18	62	M	84	26	8	120	1.18	10	47.3
19	57	M	94	24	7	120	1.38	0	26.6
20	79	M	18	24	61	1.41	0.97	23.6	33.3
Healthy									
1	56	F							
2	54	F							
3	68	M							
4	66	F							
5	64	M							
6	51	F							
7	53	F							
8	64	M							
9	64	M							
10	59	M							
11	61	F							
12	77	F							

y: years, M: male, F: female, mo: months, MOCA: Montreal Cognitive Assessment, FM: Fugl-Meyer, WMFT: Wolf Motor Function Test, s: seconds, kg: kilograms.

the principal eigenvector (λ_1) and may reflect axonal properties within white matter (Budde et al., 2009; Zhang et al., 2009). RD is a measure of diffusion orthogonal to the principal eigenvector, calculated as the average of the second and tertiary eigenvalues ($\lambda_2 + \lambda_3 / 2$) and may be related to properties of the myelin sheath (Song et al., 2003; Zhang et al., 2009). Approximate fiber tract volume was also recorded and stored for further analysis. The same measures were also extracted for whole-brain reconstructed fiber tracts.

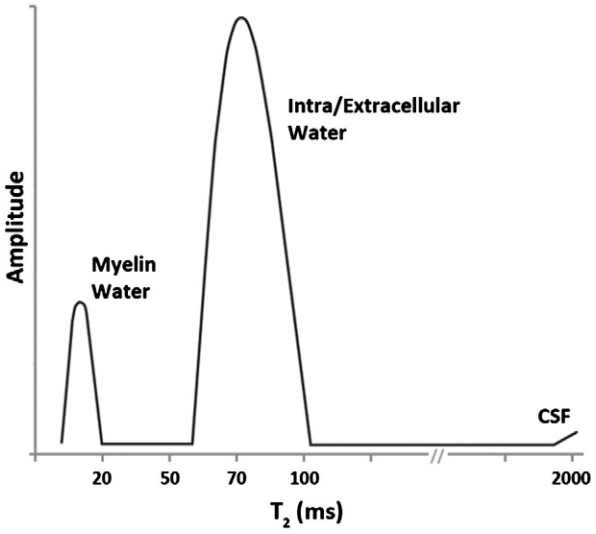

Fig. 2. Schematic example of a typical T_2 distribution from human white matter illustrating the components of the signal attributed to different tissue water environments based on relaxation time.

2.4. Behavioral assessment of upper extremity motor behavior

Participants in the stroke group completed a comprehensive battery of assessments to quantify motor behavior during the chronic phase of recovery. These assessments were administered by a licensed physical therapist (M.R.B). In addition to the FM test to index upper extremity motor impairment level, motor function was measured using the Wolf Motor Function Test (WMFT). The WMFT has been shown to be a reliable and valid assessment of upper extremity motor function in stroke (Wolf et al., 2005). Testing consisted of fifteen timed movement tasks and two tests of strength. Movement time for each task was averaged over three trials and median movement time was calculated across all tasks. Data were then log-transformed for parametric statistical analyses. Maximum grip strength was averaged over three trials using a calibrated hydraulic handheld dynamometer (Jamar, Lafayette Instrument, Lafayette, IN, USA).

2.5. Statistical analyses

All dependent measures were assessed to ensure normality prior to parametric statistical testing. If a measure was found to violate the assumptions of normality, non-parametric tests were applied. Test/re-test (mean time between scans: 224.1 days, range: 106–422 days) and inter-rater reliability were assessed in a subset ($n = 10$) of participants in the stroke group. To assess inter-rater reliability of subject-specific manual ROI delineation, a second blinded rater manually delineated the PLIC bilaterally. Intraclass correlation coefficients (ICCs) were

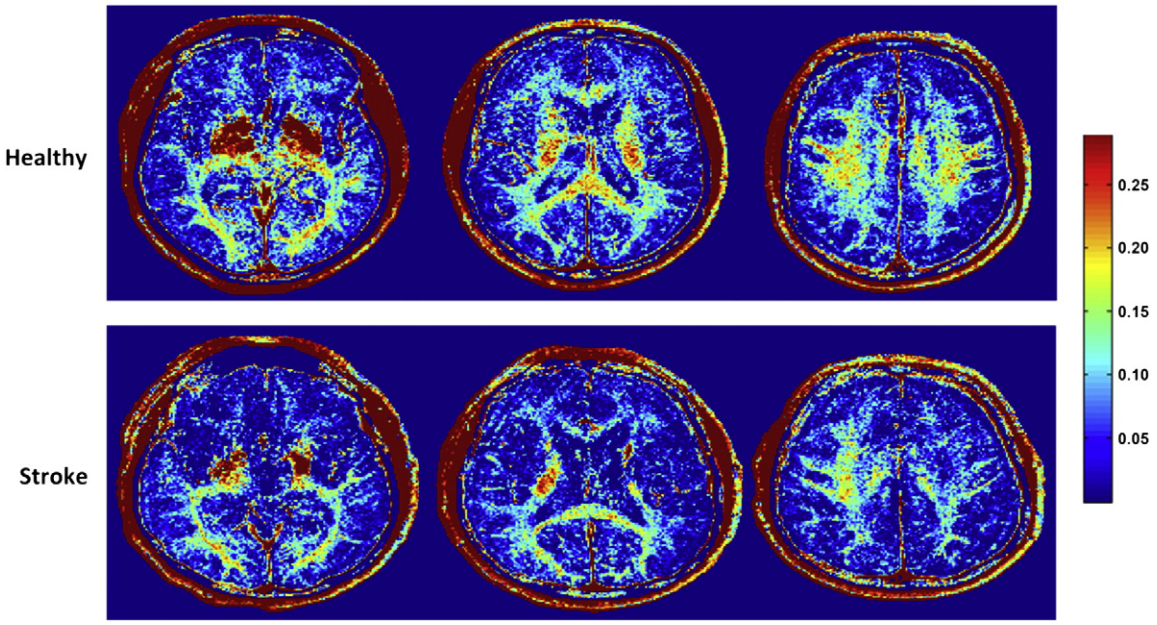

Fig. 3. Representative slices from myelin water fraction (MWF) maps of a healthy participant (HC08) (top panel) and an individual with stroke (S09) (bottom panel). Note both local and global reductions in white matter MWF for the stroke participant compared to healthy control.

calculated for MWF values within each ROI using separate two-way mixed effect models where test and rater effects were random and measure effects of individual ratings were fixed (Shrout and Fleiss, 1979). ICC values greater than 0.75 were considered to indicate excellent reliability while values between 0.40 and 0.75 demonstrated fair to good reliability and less than 0.40 were indicative of poor reliability (Rosner, 2005). Manual ROI identification in stroke has been shown to be sensitive to change in white matter after stroke and a reliable approach to quantify white matter tissue status in healthy individuals and in chronic stroke using DTI techniques (Borich et al., 2012b; Qiu et al., 2011; Stinear et al., 2007).

A between-group multivariate analysis of variance (MANOVA) was conducted to assess differences in MCRI measures of white matter (MWF, I/E GMT_2, I/EWF, GMT_2) between healthy individuals and individuals with stroke for each ROI. A second between-group MANOVA was conducted using DTI-based measures of diffusion characteristics (tract volume, FA, MD, AD, RD) as the dependent variables. Ipsilesional PLIC values were compared to non-dominant (right) PLIC values to account for potential use-dependent differences in white matter content in healthy controls. Follow-up univariate ANOVAs were conducted to assess group differences for each measure individually and a 95% confidence interval (CI) was used to quantify point estimate precision.

Bivariate correlations were conducted to evaluate relationships between white matter MWF and measures of diffusion behavior (FA, MD, AD, RD) in the PLIC bilaterally for each group. A second correlational analysis was conducted for measures of motor behavior (FM score, log-transformed WMFT score, grip strength) with MWF and FA for each ROI in the stroke group. Due to the exploratory nature of this correlational analysis, we chose to only use one primary MCRI-based and DTI-based measure to minimize multiple comparisons. An uncorrected

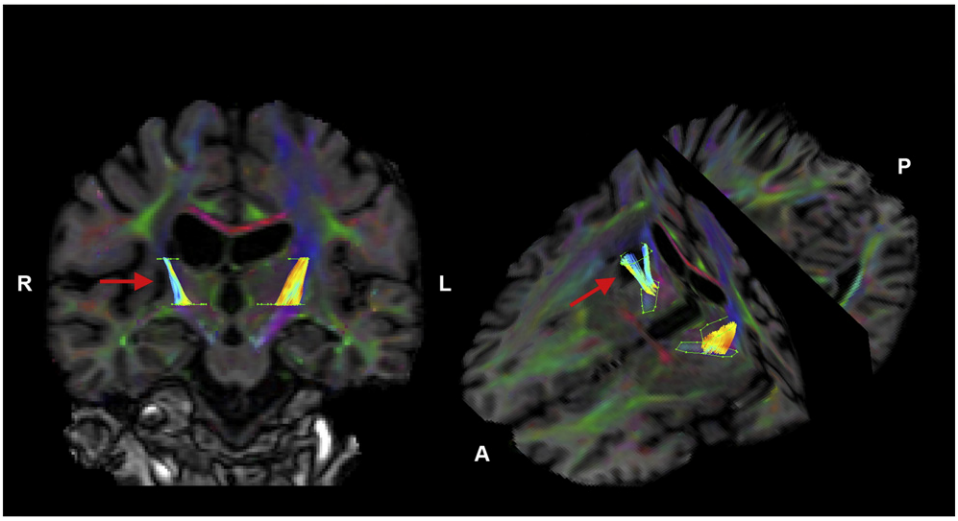

Fig. 4. Example of tract segment approach used to quantify diffusion behavior within the posterior limb of internal capsule (PLIC) bilaterally in a participant with stroke (S08). Reconstructed fiber tracts in the PLIC are color-coded by fractional anisotropy value where warmer colors represent higher values. Red arrow indicates stroke lesion location.

two-tail significance level was used for correlational analyses and set to $p < 0.05$. All statistical procedures were conducted using SPSS software (SPSS 19.0).

3. Results

3.1. Reliability of MWF in stroke

Good to excellent test/re-test reliability was observed for each ROI (ICC range: 0.70–0.98). Excellent inter-rater reliability was observed for manual delineation of the PLIC bilaterally (ICCs: ipsilesional: 0.91, contralesional: 0.87). Results summarized in Table 2.

3.2. Changes in T_2 relaxation parameters after stroke

Table 3 summarizes *in vivo* results for MWF, I/E GMT_2, I/EWF and global GMT_2 for each ROI (NAWM, RPLIC and LPLIC). MANOVA results demonstrated significant differences in T_2 relaxation measurements in the stroke group in whole-cerebrum NAWM (Wilks' $\lambda = .466$, $F_{(4,27)} = 7.75$, $p = 0.0002$, partial $\eta^2 = .534$) with reduced MWF ($p = 0.0003$) and increased I/E GMT_2 ($p = 0.01$), I/EWF ($p = 0.012$) and GMT_2 ($p < 0.0001$) values. Significant differences in overall T_2 relaxation parameters were not observed in the ipsilesional (Wilks' $\lambda = .757$, $F(4,27) = 2.16$, $p = .100$, partial $\eta^2 = .243$) nor contralesional (Wilks' $\lambda = .833$, $F(4,27) = 1.36$, $p = .276$) PLIC compared to non-dominant and dominant PLIC regions respectively in healthy participants. Follow-up analyses revealed significantly reduced MWF values in both the ipsilesional ($p = .017$, $CI_{95\%}$: 0.005–0.05) and contralesional ($p = 0.037$, $CI_{95\%}$: 0.001–0.038) PLIC (Fig. 5).

3.3. Changes in diffusion characteristics after stroke

Table 4 summarizes the results for tract volume, mean FA, mean MD, mean AD and mean RD for each region of reconstructed fiber tracts (whole-brain, bilateral PLIC). No fiber tracts were successfully reconstructed in the ipsilesional PLIC for three participants in the stroke group due to lesion encroachment. MANOVA results demonstrated significant differences in DTI-based metrics in the stroke group in whole-brain fiber tracts (Wilks' λ: .405, $F(5, 25) = 7.346$, $p < 0.0005$, partial $\eta^2 = .595$) with reduced tract volume ($p < 0.0005$) and FA ($p = 0.032$) and increased MD, AD, and RD (all $p < 0.0005$) values. Significant differences in diffusion characteristics were observed in the ipsilesional PLIC (Wilks' $\lambda = .440$, $F(4,23) = 2.16$, $p = 0.001$, partial $\eta^2 = .560$) and a trend for a difference in the contralesional PLIC (Wilks' $\lambda = .711$, $F(4,26) = 2.642$, $p = 0.056$, partial $\eta^2 = .289$) compared to non-dominant and dominant PLIC regions in healthy participants. Follow-up analyses revealed significantly reduced FA values ($p = 0.003$) and increased MD, AD and RD values ($p < 0.0005$) in the ipsilesional PLIC. In the contralateral PLIC, increased MD ($p = 0.009$) and RD ($p = 0.029$) were observed.

Table 2
Test/re-test and intra reliability of myelin water fraction in a subset of participants with stroke.

ROI	Reliability analysis	Cronbach's α	ICC (±$CI_{95\%}$)	F test	df	p value
	Test/re-test					
Whole-cerebrum NAWM		0.96	0.92 (0.70–0.98)	22.47	9	<0.0001*
Contralesional PLIC		0.83	0.70 (0.17–0.92)	5.71	9	0.008*
Ipsilesional PLIC		0.99	0.98 (0.92–0.99)	100.48	9	<0.0001*
	Inter-rater					
Contralesional PLIC		0.93	0.87 (0.57–0.97)	14.73	9	<0.0001*
Ipsilesional PLIC		0.95	0.91 (0.69–0.98)	21.89	9	<0.0001*

ROI: region of interest, ICC: Intraclass correlation coefficient, CI: confidence interval, df: degrees of freedom, NAWM: normal-appearing white matter, PLIC: posterior limb internal capsule.
* $p < 0.05$.

3.4. Relationship between myelin water fraction and diffusion characteristics

Table 5 summarizes the results of the bivariate correlation analysis between MWF and measures of diffusion (FA, MD, AD, RD). A significant relationship between MWF and measures of diffusion was not observed (all $p > 0.05$) in either group for PLIC ROIs. Regional relationships between MWF and DTI-based metrics for both groups are also represented graphically (Fig. 6).

3.5. Relationship between MWF, FA and motor behavior

Table 6 provides a summary of the correlation results between measures of white matter (MWF, FA) and motor behavior (FM score, WMFT score, grip strength) across ROIs in the stroke group. Ipsilesional PLIC mean FA was the only measure significantly correlated ($p < 0.05$) with motor behavior (FM score) in the chronic stroke group. Motor behavior was not significantly correlated with MWF values in any of the ROIs, including ipsilesional PLIC (Fig. 7).

4. Discussion

We investigated *in vivo* myelin and intra/extracellular water in brain white matter tissue following stroke using quantitative multi-echo T2 imaging. Three-dimensional MCRI of the human brain now permits the quantitative assessment of different tissue water environments *in vivo*. Importantly, recent advances in this technique now offer the opportunity to investigate these novel properties of whole-cerebrum white matter structure in clinically feasible acquisition times, enabling the study of clinical populations. Here, we also report changes in diffusion characteristics that have been previously observed in chronic stroke. Significant relationships between MWF and DTI-based metrics in the PLIC were not observed for either group. A weak relationship was observed between diffusion behavior and level of upper extremity physical impairment whereas MWF in the region of ipsilesional descending motor output tracts was not correlated with measures of motor behavior in chronic stroke.

Past investigations of white matter pathology have relied heavily on diffusion imaging techniques that have shown white matter integrity reductions in stroke, indicated by lower FA values or total fiber number, in descending motor output tracts comprising the PLIC (Lindenberg et al., 2010; Qiu et al., 2011; Stinear et al., 2007). An advantage of diffusion imaging approaches is the ability to infer directionality of white matter fiber tracts; additionally tractography can be used to reconstruct fiber tracts connecting brain regions. However, traditional DTI modeling is not accurate in areas of complex architecture that demonstrate partial volume effects thus affecting interpretation of diffusion tensor-based metrics (Alexander et al., 2001; Pierpaoli et al., 1996; Vos et al., 2012). The importance of this limitation was underscored in recent work demonstrating that crossing fibers are present in ~90% of brain white matter voxels (Jeurissen et al., 2010). Also, DTI provides gross information regarding the microstructural integrity of white matter that may be influenced by a number of factors including: axonal packing density, axonal membrane status, myelin thickness or neuronal cytoarchitectural properties (Alexander et al., 2007) making it challenging to assign changes in diffusion-based metrics of microstructural properties of white matter to specific tissue components. There are other diffusion-based analysis techniques becoming clinically feasible that have been proposed to address the challenges of complex white matter architecture and potentially improve the specificity of diffusion-based measures (Jensen

Table 3
In vivo myelin water fraction (MWF), intra/extracellular geometric mean T_2 (I/E GMT_2), intra/extracellular water fraction (I/EWF), and global GMT_2 for each group and region of interest (standard deviation).

		MWF	I/E GMT_2 (ms)	I/EWF	GMT_2
NAWM					
	Stroke	0.112 (0.012)	74.4 (2.5)	0.877 (0.013)	67.0 (2.7)
	Healthy	0.130 (0.011)	72 (2.1)	0.864 (0.012)	62.8 (1.6)
	% difference of stroke relative to healthy	−13.8*	3.3*	1.5*	6.7*
PLIC					
Contralesional	Stroke	0.162 (0.024)	73.3 (2.7)	0.819 (0.020)	61.8 (2.8)
Dominant	Healthy	0.182 (0.027)	72.5 (2.2)	0.809 (0.027)	60.1 (2.8)
	% difference of stroke relative to healthy	−10.0*	1.1	1.2	2.8
Ipsilesional	Stroke	0.153 (0.031)	73.5 (6.0)	0.812 (0.055)	67.4 (12.2)
Non-dominant	Healthy	0.181 (0.027)	72.3 (2.6)	0.809 (0.028)	60.3 (2.9)
	% difference of stroke relative to healthy	−14.9*	1.7	0.4	11.8

NAWM: normal appearing white matter, PLIC: posterior limb of internal capsule.
* $p < .05$.

et al., 2005; Jeurissen et al., 2011; Pasternak et al., 2008; Tournier et al., 2008; Wang et al., 2011).

Here, we applied a novel whole-cerebrum MCRI technique to extract components of the T_2 relaxation signal in order to examine the status of specific tissue water compartments in the stroke-affected brain. This imaging method provides a histopathologically-validated quantification of myelin content. Previous co-application of these techniques has shown that MCRI and DTI at 3T are correlated in healthy individuals in certain brain white matter regions (major and minor forceps) and uncorrelated in others (genu and splenium of corpus callosum) (Mädler et al., 2008). Our results suggest that MWF and DTI-base metrics are not strongly correlated when evaluating white matter status within the PLIC in individuals with stroke or healthy controls. Taken together, MCRI offers information regarding tissue properties not available with more common neuroimaging approaches such as DTI and as such, enables new opportunities to study the pathophysiology of, and recovery from, stroke.

Our results demonstrate that even in the chronic stage after stroke, myelin is widely disrupted with reductions extending well beyond ipsilesional structures. We also show altered intra/extracellular water fraction and geometric mean T_2 times of intra/extracellular water in the chronic phase of recovery after stroke. This supports the previous diffusion imaging work showing that changes in diffusivity secondary to cerebral ischemia are associated with changes in tissue water that can persist into the chronic phase of stroke (Sotak, 2004). Taken together these results suggest that stroke has a broad, disruptive effect on brain white matter tissue that persists into the chronic phase of recovery. Importantly, our demonstration of *in vivo* quantification of myelin illustrates a new method by which specific changes, *i.e.*, myelin health, may be tracked across the trajectory of recovery.

Results of the present study demonstrate reductions in myelin water fraction after stroke in regions both local and remote to the area of infarct compared to control participants. Previous work shows that white matter and neuronal supporting cells such as myelin-producing oligodendrocytes are particularly vulnerable to ischemia in part due to the lower blood flow under normal conditions compared to gray matter regions (Lo et al., 2003; Pantoni et al., 1996). Longitudinal studies using conventional imaging techniques have also shown that white matter infarcts can both progress and enlarge (Gouw et al., 2008) which may be exacerbated under circumstances of chronic hypoperfusion associated with long-term hypertension, a significant stroke risk factor. Wallerian degeneration, anterograde degeneration to axons and myelin sheaths due to proximal cell body or axonal injury (Werring et al., 2000), is another potential mechanism associated with stroke pathophysiology that could explain the observed results. Our DTI results suggest multiple potential loci for local and remote pathophysiologic changes following stroke. Given current technological limitations, we are unable to distinguish the relative contributions of these contributing factors, however it is conceivable that each plays some role in the substantial stroke related changes in white matter noted in our data.

Another potential factor contributing to reduced whole brain myelin water after stroke may be use-dependent neuroplastic changes in response to physical inactivity. Aerobic exercise, cognitive training and motor skill practice are associated with positive changes in both brain structure and behavior. In contrast, periods of immobilization or inactivity have been linked to adverse neuroplastic change. Experience-dependent plasticity has been demonstrated in both healthy rodents (Kleim et al., 2002) and primates (Nudo et al., 1996) and remains present even after ischemic infarcts (Nudo and Milliken, 1996). The relationship between activity level and microstructural change has also been observed in regions of white matter of healthy adult humans using DTI to quantify response to cognitive and motor training paradigms (Lovden et al., 2010; Scholz et al., 2009). Importantly, both the healthy and damaged brain appear to maintain the capacity for positive adaptive white matter plasticity including oligodendrogenesis and (re)myelination in response to experience and/or injury (Franklin and Ffrench-Constant, 2008; Markham and Greenough, 2004). However, recent data suggest that the opposite is also possible; significant disuse or inactivity may lead to reductions in white matter microstructure that extend beyond the initial stroke-related losses in brain tissue.

The impact of inactivity on brain organization may involve demyelination and reduced synaptic connectivity. This has been tested experimentally using upper extremity immobilization to focally reduce sensory input and motor output, two key components of use-dependent plasticity. After at least two weeks of immobilization secondary to humerus or elbow fracture without neurologic injury, individuals demonstrate reduced white matter integrity and cortical thickness in the contralateral motor output pathway (Langer et al., 2012). In this paradigm, forced use of the non-immobilized hand led to mirror increases in white matter integrity and cortical thickness of the opposite hemisphere (Langer et al., 2012). After stroke, hemiparesis can reduce the use of the affected extremities (Lang et al., 2007) and can also lead to decreases in overall activity that could have widespread consequences for brain white matter plasticity, especially during the chronic phase of recovery. It has been shown that physical activity level, quality of life and motor function tend to decrease with increasing time since stroke onset during the chronic phase of recovery (Edwards et al., 2010).

Lastly, premorbid inactivity may have been a predisposing factor for stroke occurrence in our participants. In theory, this lack of use may have also been a contributing factor to the widespread changes in myelin water content after stroke. Due to the cross-sectional nature of this investigation, these explanations cannot be confirmed

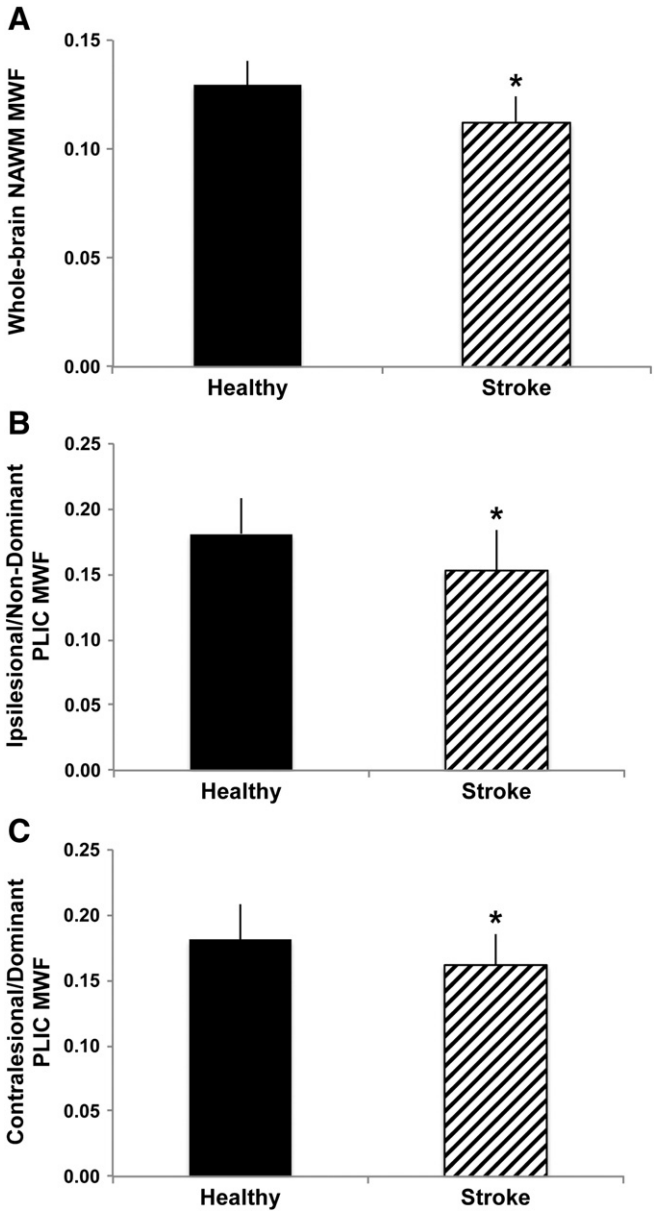

Fig. 5. Group differences in myelin water fraction (MWF) between healthy controls and participants with chronic stroke. MWF was significantly reduced in whole-cerebrum normal appearing white matter (NAWM) in the stroke group compared to whole-cerebrum NAWM in the healthy group (A), in the ipsilesional posterior limb of internal capsule (PLIC) and non-dominant PLIC MWF in the healthy group (B) and in the contralesional PLIC for the stroke group *versus* dominant PLIC in the healthy group (C) (*$p < 0.05$). Error bars represent standard deviation.

but future work could employ a longitudinal design with measures of premorbid and current activity level collected to provide further insights into the interplay between stroke, white matter status and experience-dependent plasticity.

MCRI has been used to evaluate myelin content in patients with MS (Laule et al., 2004), phenylketonuria (Sirrs et al., 2007) and schizophrenia (Flynn et al., 2003); recent work demonstrated a relationship between clinical disability scores and MWF in individuals with MS (Laule et al., 2011). In the present study, MWF was not associated with level of motor function or degree of physical impairment in the chronic phase of recovery from stroke. In patients with MS, MWF has been quantified in both lesions and NAWM whereas we chose normal appearing whole-cerebrum white matter and white matter regions previously shown to have altered white matter microstructure after stroke that were associated with motor function and response to training (Borich et al., 2012a; Stinear et al., 2007). Additionally, differences in the psychometric properties of the clinical assessments performed in MS *versus* stroke may explain, in part, the lack of a relationship between MWF and motor recovery after stroke. Lastly, chronic changes in tissue water environments after stroke may be fundamentally different than those observed in active MS lesions. To verify that the changes we noted in white matter brain structure were not a side effect of spontaneous recovery from stroke it was important to examine individuals who had stable function and brain structure, hence we studied individuals in the chronic stage. Despite the extended length of time after stroke we noted persistent changes in MWF and intra/extracellular water. We did observe a relationship between ipsilesional PLIC FA and level of upper extremity motor impairment (FM score) supporting previous investigations demonstrating a significant link between white matter status and motor function in chronic stroke (Qiu et al., 2011; Schaechter et al., 2009; Stinear et al., 2007). These results may suggest that in white matter tissue regions associated with ipsilesional descending motor output pathways that other microstructural changes contribute to motor impairments in chronic stroke. Determining the microstructural correlates of motor behavior in individuals with chronic stroke was not the primary aim of this investigation but our preliminary results support further investigation to determine the functional significance of changes in white matter tissue after stroke.

Here we chose not to formally examine lesions directly due to the heterogeneity of location, size and tissue type within the stroke group in the size of sample studied and the limitation of replicating the lesion region of interest in the healthy control group. However, exploratory analyses of lesion ROIs were performed that demonstrated significant heterogeneity in MCRI-based measures of tissue compartment water. The underlying mechanism for this heterogeneity in T_2 behavior is currently unknown but future inquiries with larger sample sizes and additional measurement techniques may prove useful to explicitly characterize differences in lesion composition during the chronic phase of recovery.

This study has some limitations. As mentioned previously, the cross-sectional design restricts our ability to draw causal inferences from observed differences in white matter T_2 relaxation measures between individuals with stroke and healthy controls and limits the ability to characterize changes in these measures over time. Widespread reductions in whole-cerebrum normal-appearing white matter MWF may have been present prior to infarct and could be associated with factors associated with increased risk of stroke (*e.g.* hypertension, diabetes, obesity, smoking, physical inactivity). This could be assessed using a longitudinal pre/post design but would require large recruitment sample sizes that are not normally feasible. Given that we have now shown that MCRI can demonstrate widespread changes in white matter myelin content and tissue water environments that were not evident previously, a longitudinal study is now justified to consider these questions. In addition, we chose to manually delineate the PLIC bilaterally rather than to apply automated approaches define our regions of interest. Although we demonstrated excellent inter-rater reliability for manual ROI determination, there is the potential that this approach could have introduced variability into the data. However, this technique has previously been shown to be reproducible between raters and ratings using DTI-derived image maps (Borich et al., 2012b) and it enabled us to account for each individual's anatomy in the presence of heterogeneous lesion size and location. In addition, previous investigations using MCRI-based MWF measurement have employed ROI-based methods to evaluate myelin water content in brain and cervical spinal cord (Laule et al., 2004, 2006; MacMillan et al., 2011; Prasloski et al., 2012b) We also evaluated an objectively defined ROI determined using automatic brain segmentation techniques to produce a whole-cerebrum normal appearing white matter ROI. However, ROI-based analysis approaches may miss other regions affected by stroke that could have stronger associations with motor recovery

Table 4
Tract volume, mean fractional anisotropy (FA), mean diffusivity (MD), axial diffusivity (AD) and radial diffusivity (RD) for each group for reconstructed fiber tracts within each region of interest (standard deviation).

		Tract volume	FA	MD	AD	RD
Whole-brain fiber tracts						
	Stroke	246.23 (51.82)	0.488 (0.012)	0.882 (0.035)	1.41 (0.04)	0.617 (0.032)
	Healthy	327.94 (42.90)	0.498 (0.010)	0.827 (0.170)	1.34 (0.02)	0.572 (0.017)
	% difference of stroke relative to healthy	−25.0**	−2.0*	6.2**	5.0**	7.3**
PLIC fiber tract segment						
Contralesional	Stroke	1.10 (0.41)	0.632 (0.050)	0.756 (0.050)	1.41 (0.06)	0.443 (0.061)
Dominant	Healthy	1.26 (0.14)	0.662 (0.040)	0.719 (0.032)	1.37 (0.05)	0.395 (0.042)
	% difference of stroke relative to healthy	−12.7	−4.5	6.4**	2.9	10.8*
Ipsilesional	Stroke	0.92 (0.92)	0.552 (0.0832)	0.910 (0.514)	1.54 (0.016)	0.597 (0.163)
Non-dominant	Healthy	1.14 (0.26)	0.640 (0.036)	0.747 (0.026)	1.39 (0.040)	0.428 (0.039)
	% difference of stroke relative to healthy	−19.3	−13.8**	17.9**	9.7**	28.3**

PLIC: posterior limb of internal capsule. Tract volume shown in units 10^3 mm^3. MD, AD and RD are units 10^{-3} mm^2/s.
* $p < 0.05$.
** $p < 0.01$.

Table 5
Correlation coefficients between measures of diffusion and myelin water fraction in the posterior limb of internal capsule.

		FA	MD	AD	RD
		r	*r*	*r*	*r*
MWF					
Stroke	Contralesional	0.13	−0.16	−0.04	−0.18
	Ipsilesional	0.28	−0.33	−0.29	−0.32
Healthy	Dominant	0.07	−0.38	−0.43	−0.17
	Non-dominant	−0.08	0.32	0.30	0.16

FA: fractional anisotropy, MD: mean diffusivity, AD: axial diffusivity, RD: radial diffusivity, MWF: myelin water fraction, $p > 0.05$.

than the regions selected. The regions evaluated were chosen *a priori* based on previous white matter imaging studies in stroke (Qiu et al., 2011; Stinear et al., 2007) and to minimize the potential for type I error associated with multiple ROI comparisons. Future work may benefit from the use of voxel-based or multimodal imaging techniques to explore other local and/or distributed brain regions and networks that may demonstrate changes in other tissue water environments. However despite advances in spatial normalization approaches in stroke, it remains challenging to use voxelwise approaches that rely on normalization of lesioned brains to a common space in order to identify common regions of microstructural change after stroke, especially in the context of heterogenous lesion location and size found in our stroke cohort. Combining *in vivo* myelin water mapping with other imaging techniques could offer new multimodal imaging paradigms to consider the relationship of

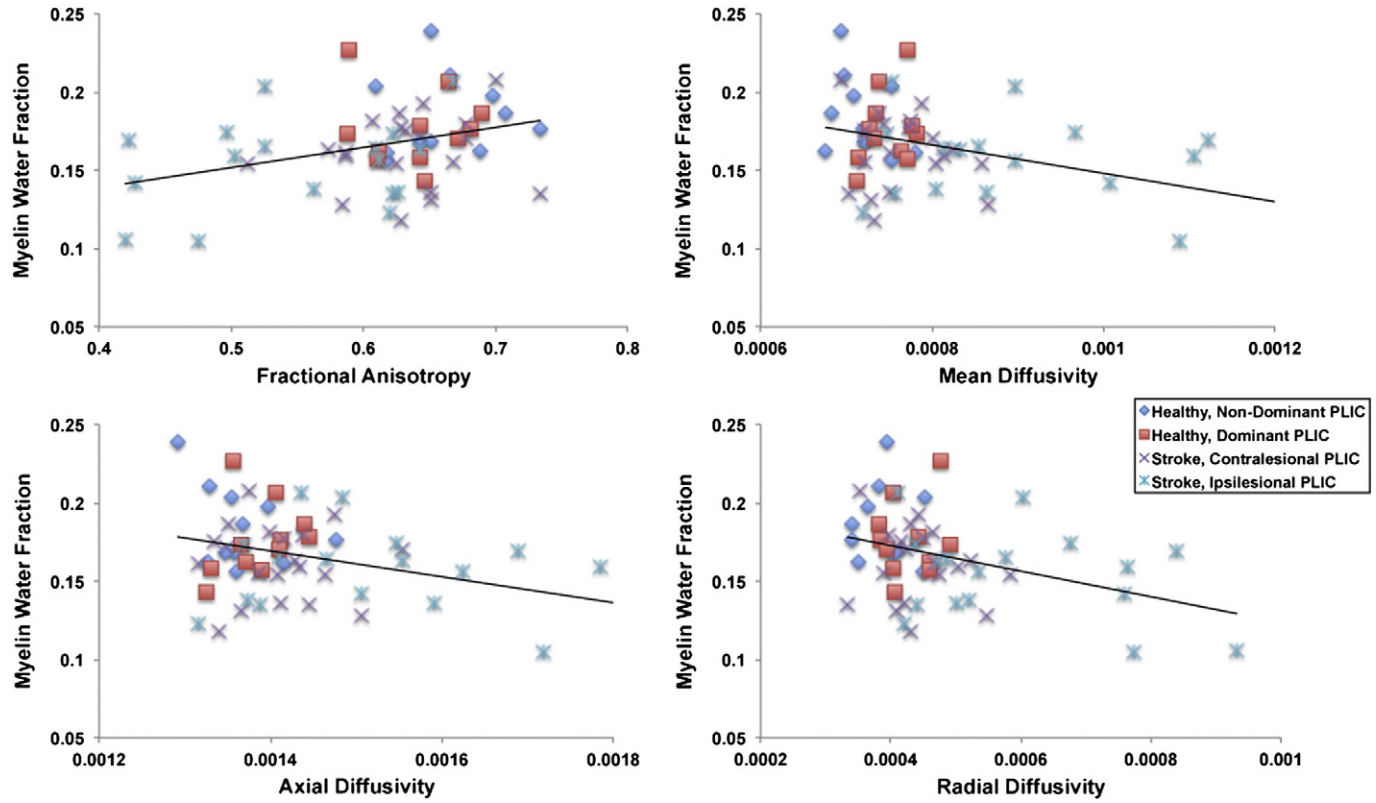

Fig. 6. Scatter plots depicting the relationship between myelin water fraction (MWF) and measures of diffusion behavior in the posterior limb of internal capsule (PLIC) across participants. Myelin water fraction was not significantly correlated with diffusion behavior within the PLIC for either group, ($p > 0.05$).

Table 6
Summary of correlation results between measures of motor behavior with myelin water fraction and fractional anisotropy in white matter regions of interest in the stroke group.

	FM score		Log WMFT affected		Log WMFT unaffected		Grip strength affected		Grip strength unaffected	
	r	p value	*r*	p value	*r*	p value	*r*	p value	*r*	p value
MWF										
NAWM	−0.05	0.82	0.44	0.65	0.09	0.70	−0.05	0.84	0.08	0.73
Contralesional PLIC	−0.43	0.06	0.43	0.06	0.11	0.64	−0.34	0.15	0.01	0.95
Ipsilesional PLIC	0.08	0.73	−0.04	0.87	−0.23	0.33	0.15	0.52	0.04	0.85
FA										
Whole-brain	0.02	0.82	0.09	0.69	−0.29	0.22	−0.02	0.92	0.37	0.10
Contralesional PLIC	−0.11	0.64	0.11	0.66	−0.07	0.76	−0.30	0.20	0.20	0.40
Ipsilesional PLIC	0.51	0.04*	−0.47	0.096	0.14	0.59	0.07	0.79	−0.70	0.79

FM: Fugl-Meyer, WMFT: Wolf Motor Function Test, NAWM: Normal appearing white matter, PLIC: posterior limb of internal capsule, MWF: myelin water fraction, FA: fractional anisotropy.
* $p<0.05$.

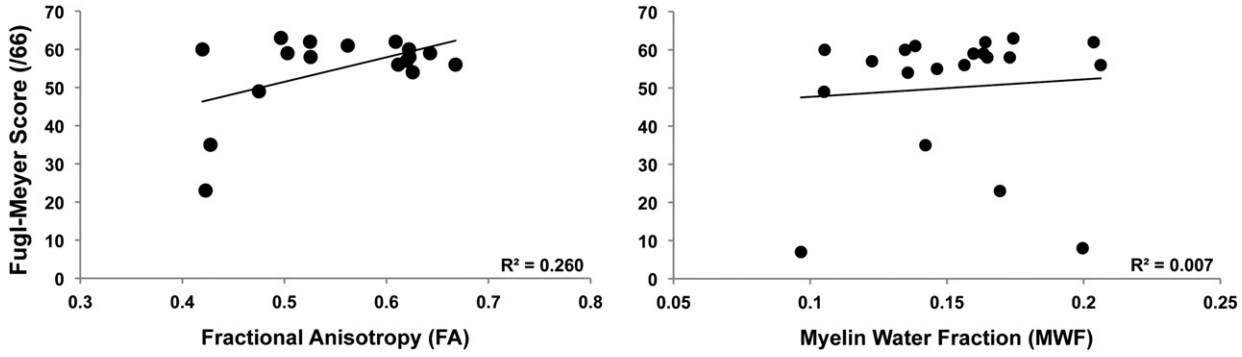

Fig. 7. Scatter plots depicting the relationship between fractional anisotropy (FA) and myelin water fraction (MWF) with the ipsilesional PLIC and level of physical impairment represented by upper extremity Fugl-Meyer (FM) score. A significant correlation was observed between FA and FM score ($p = 0.04$) but not between MWF and FM score ($p = 0.365$).

tissue-specific white matter characteristics with measures of neural activity and functional connectivity. This work may provide additional novel insights into stroke pathology and potentially offer novel biomarkers to predict the trajectory of recovery and response to therapeutic intervention after stroke.

5. Conclusions

This is the first report of 3D, multi-component T_2 relaxation imaging used to reliably demonstrate differences in myelin water and other white matter tissue water environments *in vivo* after stroke. It is also the first to evaluate the relationships between MWF with diffusion behavior and motor function following stroke. Future investigations should determine the clinical utility of these parameters across the time course of recovery from stroke and other neurologic disorders.

Acknowledgments

This work was supported by the Canadian Institutes of Health Research [MOP-1066551 to L.A.B]. MRB received salary support from the Heart and Stroke Foundation of Canada. LAB is supported by the Canada Research Chairs and Michael Smith Foundation for Health Research. AR is supported by the CIHR New Investigator Program and NSERC. We would like to acknowledge David K. Li for his comments that have improved the clarity of this work. We would also like to thank Monika McKeown for her assistance with the data processing. We wish to acknowledge the continuing research support from Philips Healthcare.

References

Alexander, A.L., Hasan, K.M., Lazar, M., Tsuruda, J.S., Parker, D.L., 2001. Analysis of partial volume effects in diffusion-tensor MRI. Magnetic Resonance in Medicine 45, 770–780.
Alexander, A.L., Lee, J.E., Lazar, M., Field, A.S., 2007. Diffusion tensor imaging of the brain. Neurotherapeutics 4, 316–329.
Assaf, Y., Basser, P.J., 2005. Composite hindered and restricted model of diffusion (CHARMED) MR imaging of the human brain. NeuroImage 27, 48–58.
Baumann, N., Pham-Dinh, D., 2001. Biology of oligodendrocyte and myelin in the mammalian central nervous system. Physiological Reviews 81, 871–927.
Borich, M.R., Mang, C., Boyd, L.A., 2012a. Both projection and commissural pathways are disrupted in individuals with chronic stroke: investigating microstructural white matter correlates of motor recovery. BMC Neuroscience 13 (1), 107 (Aug 29).
Borich, M., Wadden, K., Boyd, L., 2012b. Establishing the reproducibility of two approaches to quantify white matter tract integrity in stroke. NeuroImage 59, 2393–2400.
Budde, M.D., Xie, M., Cross, A.H., Song, S.-K., 2009. Axial diffusivity is the primary correlate of axonal injury in the experimental autoimmune encephalomyelitis spinal cord: a quantitative pixelwise analysis. The Journal of Neuroscience 29, 2805–2813.
Chang, L.C., Jones, D.K., Pierpaoli, C., 2005. RESTORE: robust estimation of tensors by outlier rejection. Magnetic Resonance in Medicine 53, 1088–1095.
Chida, Y., Kokubo, Y., Sato, S., Kuge, A., Takemura, S., Kondo, R., Kayama, T., 2011. The alterations of oligodendrocyte, myelin in corpus callosum, and cognitive dysfunction following chronic cerebral ischemia in rats. Brain Research 1414, 22–31.
Cramer, S.C., 2008. Repairing the human brain after stroke: I. Mechanisms of spontaneous recovery. Annals of Neurology 63, 272–287.
Deoni, S.C.L., Rutt, B.K., Arun, T., Pierpaoli, C., Jones, D.K., 2008. Gleaning multicomponent T1 and T2 information from steady-state imaging data. Magnetic Resonance in Medicine 60, 1372–1387.
Dewar, D., Yam, P., McCulloch, J., 1999. Drug development for stroke: importance of protecting cerebral white matter. European Journal of Pharmacology 375, 41–50.
Edwards, J.D., Koehoorn, M., Boyd, L.A., Levy, A.R., 2010. Is health-related quality of life improving after stroke? A comparison of health utilities indices among Canadians with stroke between 1996 and 2005. Stroke 42 (5), 996–1000.
Flynn, S.W., Lang, D.J., Mackay, A.L., Goghari, V., Vavasour, I.M., Whittall, K.P., Smith, G.N., Arango, V., Mann, J.J., Dwork, A.J., Falkai, P., Honer, W.G., 2003. Abnormalities of myelination in schizophrenia detected in vivo with MRI, and post-mortem with analysis of oligodendrocyte proteins. Molecular Psychiatry 8, 811–820.
Franklin, R.J.M., Ffrench-Constant, C., 2008. Remyelination in the CNS: from biology to therapy. Nature Reviews. Neuroscience 9, 839–855.

Fugl-Meyer, A.R., Jaasko, L., Leyman, I., Olsson, S., Steglind, S., 1975. The post-stroke hemiplegic patient: a method for evaluation of physical performance. Scandinavian Journal of Rehabilitation Medicine 7, 13–31.
Gareau, P.J., Rutt, B.K., Bowen, C.V., Karlik, S.J., Mitchell, J.R., 1999. In vivo measurements of multi-component T-2 relaxation behaviour in guinea pig brain. Magnetic Resonance Imaging 17, 1319–1325.
Gareau, P.J., Rutt, B.K., Karlik, S.J., Mitchell, J.R., 2000. Magnetization transfer and multicomponent T2 relaxation measurements with histopathologic correlation in an experimental model of MS. Journal of Magnetic Resonance Imaging 11, 586–595.
Gillum, R.F., Kwagyan, J., Obisesan, T.O., 2011. Ethnic and geographic variation in stroke mortality trends. Stroke 42, 3294–3296.
Gouw, A.A., van der Flier, W.M., Pantoni, L., Inzitari, D., Erkinjuntti, T., Wahlund, L.O., Waldemar, G., Schmidt, R., Fazekas, F., Scheltens, P., Barkhof, F., Grp, L.S., 2008. On the etiology of incident brain lacunes longitudinal observations from the LADIS study. Stroke 39, 3083–3085.
Hui, E.S., Cheung, M.M., Qi, L.Q., Wu, E.X., 2008. Towards better MR characterization of neural tissues using directional diffusion kurtosis analysis. NeuroImage 42, 122–134.
Jang, S.H., Cho, S.-H., Kim, Y.-H., Han, B.S., Byun, W.M., Son, S.-M., Kim, S.H., Lee, S.J., 2005. Diffusion anisotrophy in the early stages of stroke can predict motor outcome. Restorative Neurology and Neuroscience 23, 11–17.
Jenkinson, M., Bannister, P., Brady, M., Smith, S., 2002. Improved optimization for the robust and accurate linear registration and motion correction of brain images. NeuroImage 17, 825–841.
Jensen, J.H., Helpern, J.A., Ramani, A., Lu, H., Kaczynski, K., 2005. Diffusional kurtosis imaging: the quantification of non-Gaussian water diffusion by means of magnetic resonance imaging. Magnetic Resonance in Medicine 53, 1432–1440.
Jeurissen, B., Leemans, A., Tournier, J., Jones, D., Sijbers, J., 2010. Estimating the number of fiber orientations in diffusion MRI voxels: a constrained spherical deconvolution study. Proceedings of the International Society for Magnetic Resonance in Medicine, Stockholm, Sweden, p. 573.
Jeurissen, B., Leemans, A., Jones, D.K., Tournier, J.-D., Sijbers, J., 2011. Probabilistic fiber tracking using the residual bootstrap with constrained spherical deconvolution. Human Brain Mapping 32, 461–479.
Kelly-Hayes, M., Beiser, A., Kase, C.S., Scaramucci, A., D'Agostino, R.B., Wolf, P.A., 2003. The influence of gender and age on disability following ischemic stroke: the Framingham study. Journal of Stroke and Cerebrovascular Diseases: The Official Journal of National Stroke Association 12, 119–126.
Kleim, J.A., Barbay, S., Cooper, N.R., Hogg, T.M., Reidel, C.N., Remple, M.S., Nudo, R.J., 2002. Motor learning-dependent synaptogenesis is localized to functionally reorganized motor cortex. Neurobiology of Learning and Memory 77, 63–77.
Lang, C.E., Wagner, J.M., Edwards, D.F., Dromerick, A.W., 2007. Upper extremity use in people with hemiparesis in the first few weeks after stroke. Journal of Neurologic Physical Therapy 31, 56–63.
Langer, N., Hanggi, J., Muller, N.A., Simmen, H.P., Jancke, L., 2012. Effects of limb immobilization on brain plasticity. Neurology 78, 182–188.
Laule, C., Vavasour, I.M., Moore, G.R.W., Oger, J., Li, D.K.B., Paty, D.W., MacKay, A.L., 2004. Water content and myelin water fraction in multiple sclerosis. A T2 relaxation study. Journal of Neurology 251, 284–293.
Laule, C., Leung, E., Lis, D.K.B., Traboulsee, A.L., Paty, D.W., MacKay, A.L., Moore, G.R.W., 2006. Myelin water imaging in multiple sclerosis: quantitative correlations with histopathology. Multiple Sclerosis 12, 747–753.
Laule, C., Vavasour, I.M., Kolind, S.H., Traboulsee, A.L., Moore, G.R.W., Li, D.K.B., MacKay, A.L., 2007. Long T-2 water in multiple sclerosis: what else can we learn from multiecho T-2 relaxation? Journal of Neurology 254, 1579–1587.
Laule, C., Kozlowski, P., Leung, E., Li, D.K.B., MacKay, A.L., Moore, G.R.W., 2008. Myelin water imaging of multiple sclerosis at 7 T: correlations with histopathology. NeuroImage 40, 1575–1580.
Laule, C., Vavasour, I.M., Leung, E., Li, D.K.B., Kozlowski, P., Traboulsee, A.L., Oger, J., Mackay, A.L., Moore, G.R.W., 2011. Pathological basis of diffusely abnormal white matter: insights from magnetic resonance imaging and histology. Multiple Sclerosis 17, 144–150.
Leemans, A., Jones, D.K., 2009. The B-matrix must be rotated when correcting for subject motion in DTI data. Magnetic Resonance in Medicine 61, 1336–1349.
Leemans, A., Jeurissen, B., Sijbers, J., Jones, D.K., 2009. ExploreDTI: a graphical toolbox for processing, analyzing and visualizing diffusion MR data. Proceedings of the 17th Annual Meeting of the International Society of Magnetic Resonance in Medicine, p. 3537.
Lenz, C., Klarhofer, M., Scheffler, K., 2012. Feasibility of in vivo myelin water imaging using 3D multigradient-echo pulse sequences. Magnetic Resonance in Medicine 68, 523–528.
Lindenberg, R., Renga, V., Zhu, L.L., Betzler, F., Alsop, D., Schlaug, G., 2010. Structural integrity of corticospinal motor fibers predicts motor impairment in chronic stroke. Neurology 74, 280–287.
Lo, E.H., Dalkara, T., Moskowitz, M.A., 2003. Mechanisms, challenges and opportunities in stroke. Nature Reviews. Neuroscience 4, 399–415.
Lovden, M., Bodammer, N.C., Kuhn, S., Kaufmann, J., Schutze, H., Tempelmann, C., Heinze, H.-J., Duzel, E., Schmiedek, F., Lindenberger, U., 2010. Experience-dependent plasticity of white-matter microstructure extends into old age. Neuropsychologia 48, 3878–3883.
Lundy-Ekman, K., 1998. Neuroscience: Fundamentals for Rehabilitation. WB Saunders, Philadelphia.
Mackay, A., Whittall, K., Adler, J., Li, D., Paty, D., Graeb, D., 1994. In-vivo visualization of myelin water in brain by magnetic resonance. Magnetic Resonance in Medicine 31, 673–677.
MacMillan, E.L., Madler, B., Fichtner, N., Dvorak, M.F., Li, D.K.B., Curt, A., MacKay, A.L., 2011. Myelin water and T-2 relaxation measurements in the healthy cervical spinal cord at 3.0T: repeatability and changes with age. NeuroImage 54, 1083–1090.
Mädler, B., Drabycz, S.A., Kolind, S.H., Whittall, K.P., MacKay, A.L., 2008. Is diffusion anisotropy an accurate monitor of myelination? Correlation of multicomponent T2 relaxation and diffusion tensor anisotropy in human brain. Magnetic Resonance Imaging 26, 874–888.
Markham, J.A., Greenough, W.T., 2004. Experience-driven brain plasticity: beyond the synapse. Neuron Glia Biology 1, 351–363.
Menon, R.S., Allen, P.S., 1991. Application of continuous relaxation-time distributions to the fitting of data from model systems and excised tissue. Magnetic Resonance in Medicine 20, 214–227.
Minino, A.M., Murphy, S.L., Xu, J., Kochanek, K.D., 2011. Deaths: final data for 2008. National Vital Statistics Reports: From the Centers for Disease Control and Prevention, 59. National Center for Health Statistics, National Vital Statistics System 1–126.
Moore, G.R.W., Leung, E., MacKay, A.L., Vavasour, I.M., Whittall, K.P., Cover, K.S., Li, D.K.B., Hashimoto, S.A., Oger, J., Sprinkle, T.J., Paty, D.W., 2000. A pathology-MRI study of the short-T2 component in formalin-fixed multiple sclerosis brain. Neurology 55, 1506–1510.
Nasreddine, Z.S., Phillips, N.A., Bedirian, V., Charbonneau, S., Whitehead, V., Collin, I., Cummings, J.L., Chertkow, H., 2005. The Montreal Cognitive Assessment, MoCA: a brief screening tool for mild cognitive impairment. Journal of the American Geriatrics Society 53, 695–699.
Nguyen, T.D., Wisnieff, C., Cooper, M.A., Kumar, D., Raj, A., Spincemaille, P., Wang, Y., Vartanian, T., Gauthier, S.A., 2012. T2prep three-dimensional spiral imaging with efficient whole brain coverage for myelin water quantification at 1.5 tesla. Magnetic Resonance in Medicine 67, 614–621.
Noguchi, K., Ogawa, T., Inugami, A., Fujita, H., Hatazawa, J., Shimosegawa, E., Okudera, T., Uemura, K., Seto, H., 1997. MRI of acute cerebral infarction: a comparison of FLAIR and T2-weighted fast spin-echo imaging. Neuroradiology 39, 406–410.
Nudo, R., Milliken, G., 1996. Reorganization of movement representations in primary motor cortex following focal ischemic infarcts in adult squirrel monkeys. Journal of Neurophysiology 75 (5), 2144–2149.
Nudo, R., Milliken, G., Jenkins, W., Merzenich, M., 1996. Use-dependent alterations of movement representations in primary motor cortex of adult squirrel monkeys. The Journal of Neuroscience 16 (2), 785–807.
Oh, J., Han, E.T., Pelletier, D., Nelson, S.J., 2006. Measurement of in vivo multicomponent T2 relaxation times for brain tissue using multi-slice T2 prep at 1.5 and 3 T. Magnetic Resonance Imaging 24, 33–43.
Oldfield, R., 1971. The assessment and analysis of handedness: the Edinburgh inventory. Neuropsychologia 9 (1), 97–113.
Pantoni, L., Garcia, J.H., Gutierrez, J.A., 1996. Cerebral white matter is highly vulnerable to ischemia. Stroke 27, 1641–1646.
Pasternak, O., Assaf, Y., Intrator, N., Sochen, N., 2008. Variational multiple-tensor fitting of fiber-ambiguous diffusion-weighted magnetic resonance imaging voxels. Magnetic Resonance Imaging 26, 1133–1144.
Pierpaoli, C., Jezzard, P., Basser, P.J., Barnett, A., Di Chiro, G., 1996. Diffusion tensor MR imaging of the human brain. Radiology 201, 637–648.
Prasloski, T., Mädler, B., Xiang, Q.-S., MacKay, A., Jones, C., 2012a. Applications of stimulated echo correction to multicomponent T2 analysis. Magnetic Resonance in Medicine 67, 1803–1814.
Prasloski, T., Rauscher, A., MacKay, A.L., Hodgson, M., Vavasour, I.M., Laule, C., Mädler, B., 2012b. Rapid whole cerebrum myelin water imaging using a 3D GRASE sequence. NeuroImage 63, 533–539.
Qiu, M., Darling, W.G., Morecraft, R.J., Ni, C.C., Rajendra, J., Butler, A.J., 2011. White matter integrity is a stronger predictor of motor function than BOLD response in patients with stroke. Neurorehabilitation and Neural Repair 25, 275–284.
Readhead, C., Popko, B., Takahashi, N., Shine, H.D., Saavedra, R.A., Sidman, R.L., Hood, L., 1987. Expression of a myelin basic-protein gene in transgenic shiverer mice — correction of the dysmyelinating phenotype. Cell 48, 703–712.
Rosner, B., 2005. Fundamentals of Biostatistics. Duxbury Press, Belmont, CS.
Schaechter, J.D., Fricker, Z.P., Perdue, K.L., Helmer, K.G., Vangel, M.G., Greve, D.N., Makris, N., 2009. Microstructural status of ipsilesional and contralesional corticospinal tract correlates with motor skill in chronic stroke patients. Human Brain Mapping 30, 3461–3474.
Scholz, J., Klein, M.C., Behrens, T.E., Johansen-Berg, H., 2009. Training induces changes in white-matter architecture. Nature Neuroscience 12, 1370–1371.
Shrout, P., Fleiss, J., 1979. Intraclass correlations: uses in assessing rater reliability. Psychological Bulletin 2, 420–428.
Siemonsen, S., Mouridsen, K., Holst, B., Ries, T., Finsterbusch, J., Thomalla, G., Ostergaard, L., Fiehler, J., 2009. Quantitative T2 values predict time from symptom onset in acute stroke patients. Stroke 40, 1612–1616.
Siemonsen, S., Lobel, U., Sedlacik, J., Forkert, N.D., Mouridsen, K., Ostergaard, L., Thomalla, G., Fiehler, J., 2012. Elevated T2-values in MRI of stroke patients shortly after symptom onset do not predict irreversible tissue infarction. Brain 135, 1981–1989.
Sirrs, S.M., Laule, C., Madler, B., Brief, E.E., Tahir, S.A., Bishop, C., MacKay, A.L., 2007. Normal-appearing white matter in patients with phenylketonuria: water content, myelin water fraction, and metabolite concentrations. Radiology 242, 236–243.
Smith, S.M., Jenkinson, M., Woolrich, M.W., Beckmann, C.F., Behrens, T.E.J., Johansen-Berg, H., Bannister, P.R., De Luca, M., Drobnjak, I., Flitney, D.E., Niazy, R.K., Saunders, J., Vickers, J., Zhang, Y.Y., De Stefano, N., Brady, J.M., Matthews, P.M., 2004. Advances in functional and structural MR image analysis and implementation as FSL. NeuroImage 23, S208–S219.
Song, S.K., Sun, S.W., Ramsbottom, M.J., Chang, C., Russell, J., Cross, A.H., 2002. Dysmyelination revealed through MRI as increased radial (but unchanged axial) diffusion of water. NeuroImage 17, 1429–1436.
Song, S.-K., Sun, S.-W., Ju, W.-K., Lin, S.-J., Cross, A.H., Neufeld, A.H., 2003. Diffusion tensor imaging detects and differentiates axon and myelin degeneration in mouse optic nerve after retinal ischemia. NeuroImage 20, 1714–1722.
Sotak, C.H., 2004. Nuclear magnetic resonance (NMR) measurement of the apparent diffusion coefficient (ADC) of tissue water and its relationship to cell volume changes in pathological states. Neurochemistry International 45, 569–582.
Stewart, W.A., Mackay, A.L., Whittall, K.P., Moore, G.R.W., Paty, D.W., 1993. Spin-spin relaxation in experimental allergic encephalomyelitis-analysis of CPMG data using a

nonlinear least-squares method and linear inverse theory. Magnetic Resonance in Medicine 29, 767–775.
Stinear, C.M., Barber, P.A., Smale, P.R., Coxon, J.P., Fleming, M.K., Byblow, W.D., 2007. Functional potential in chronic stroke patients depends on corticospinal tract integrity. Brain 130, 170–180.
Tanaka, K., Nogawa, S., Suzuki, S., Dembo, T., Kosakai, A., 2003. Upregulation of oligodendrocyte progenitor cells associated with restoration of mature oligodendrocytes and myelination in peri-infarct area in the rat brain. Brain Research 989, 172–179.
Tournier, J.D., Yeh, C.H., Calamante, F., Cho, K.H., Connelly, A., Lin, C.P., 2008. Resolving crossing fibres using constrained spherical deconvolution: validation using diffusion-weighted imaging phantom data. NeuroImage 42, 617–625.
Vavasour, I.M., Whittall, K.P., MacKay, A.L., Li, D.K.B., Vorobeychik, G., Paty, D.W., 1998. A comparison between magnetization transfer ratios and myelin water percentages in normals and multiple sclerosis patients. Magnetic Resonance in Medicine 40, 763–768.
Vos, S.B., Jones, D.K., Jeurissen, B., Viergever, M.A., Leemans, A., 2012. The influence of complex white matter architecture on the mean diffusivity in diffusion tensor MRI of the human brain. NeuroImage 59, 2208–2216.
Wang, Y., Wang, Q., Haldar, J.P., Yeh, F.-C., Xie, M., Sun, P., Tu, T.-W., Trinkaus, K., Klein, R.S., Cross, A.H., Song, S.-K., 2011. Quantification of increased cellularity during inflammatory demyelination. Brain 134, 3590–3601.
Wang, L.E., Tittgemeyer, M., Imperati, D., Diekhoff, S., Ameli, M., Fink, G.R., Grefkes, C., 2012. Degeneration of corpus callosum and recovery of motor function after stroke: a multimodal magnetic resonance imaging study. Human Brain Mapping 33, 2941–2956.
Webb, S., Munro, C.A., Midha, R., Stanisz, G.J., 2003. Is multicomponent T-2 a good measure of myelin content in peripheral nerve? Magnetic Resonance in Medicine 49, 638–645.
Werring, D.J., Toosy, A.T., Clark, C.A., Parker, G.J., Barker, G.J., Miller, D.H., Thompson, A.J., 2000. Diffusion tensor imaging can detect and quantify corticospinal tract degeneration after stroke. Journal of Neurology, Neurosurgery, and Psychiatry 69, 269–272.
Whittall, K.P., Mackay, A.L., 1989. Quantitative interpretation of NMR relaxation. Journal of Magnetic Resonance 84, 134–152.
Whittall, K.P., MacKay, A.L., Graeb, D.A., Nugent, R.A., Li, D.K.B., Paty, D.W., 1997. In vivo measurement of T-2 distributions and water contents in normal human brain. Magnetic Resonance in Medicine 37, 34–43.
Wolf, S.L., Thompson, P.A., Morris, D.M., Rose, D.K., Winstein, C.J., Taub, E., Giuliani, C., Pearson, S.L., 2005. The EXCITE trial: attributes of the Wolf Motor Function Test in patients with subacute stroke. Neurorehabilitation and Neural Repair 19, 194–205.
Zhang, Y.Y., Brady, M., Smith, S., 2001. Segmentation of brain MR images through a hidden Markov random field model and the expectation–maximization algorithm. IEEE Transactions on Medical Imaging 20, 45–57.
Zhang, J., Jones, M., DeBoy, C.A., Reich, D.S., Farrell, J.A.D., Hoffman, P.N., Griffin, J.W., Sheikh, K.A., Miller, M.I., Mori, S., Calabresi, P.A., 2009. Diffusion tensor magnetic resonance imaging of Wallerian degeneration in rat spinal cord after dorsal root axotomy. The Journal of Neuroscience 29, 3160–3171.